Chemical Science

RSC Publishing

EDGE ARTICLE

View Article Online
View Journal | View Issue

Cite this: *Chem. Sci.*, 2013, **4**, 2453

Induced self-assembly and disassembly of water-soluble alkynylplatinum(II) terpyridyl complexes with "switchable" near-infrared (NIR) emission modulated by metal–metal interactions over physiological pH: demonstration of pH-responsive NIR luminescent probes in cell-imaging studies†

Clive Yik-Sham Chung,[a] Steve Po-Yam Li,[b] Man-Wai Louie,[b] Kenneth Kam-Wing Lo[b] and Vivian Wing-Wah Yam*[a]

Received 22nd January 2013
Accepted 11th March 2013

DOI: 10.1039/c3sc50196e

www.rsc.org/chemicalscience

Water-soluble alkynylplatinum(II) terpyridine complexes, [Pt{tpy($C_6H_4CH_2NMe_3$-4)-4′}(C≡C–Ar)](OTf)$_2$ [Ar = C_6H_3–(OH)$_2$-3,5 (**1**), C_6H_4OH-4 (**2**), C_6H_3–(OMe)$_2$-3,5 (**3**)], have been synthesized and characterized. The photophysical and electrochemical properties of the complexes have been studied. Complex **1** has been found to undergo aggregation at low pHs, leading to metal–metal and/or π–π interactions and the emergence of a triplet metal-metal-to-ligand charge transfer (^{3}MMLCT) emission in the near-infrared (NIR) region, the intensity of which has been enhanced 1350-fold over that at physiological pH. Such 'switchable' NIR emission of complex **1** was employed in cell-imaging experiments. The pH response of the ^{3}MMLCT emission of complex **1** in cellular compartments has been studied using experiments with fixed Madin–Darby canine kidney (MDCK) cells, while live cell-imaging experiments revealed that complex **1** could function as a NIR luminescent probe for the tracking of the location of acidic organelles such as lysosomes.

Introduction

Square-planar platinum(II) polypyridine complexes have attracted much attention due to their rich spectroscopic properties.[1–8] A particular class of platinum(II) complexes with long-standing interest is the alkynylplatinum(II) terpyridine complexes.[4,5] The presence of d^8–d^8 metal–metal interactions and π–π stacking of the terpyridine ligands in these complexes has led to interesting spectroscopic and luminescence properties.[4b–d,5] Recently, our group has reported the self-assembly of terpyridylplatinum(II) complexes in aqueous media induced by the addition of synthetic polyelectrolytes[4b,c,5a,d,g] as well as single-stranded nucleic acids[5c,f] and aptamers,[5f] which in turn led to remarkable UV-vis and near-infrared (NIR) emission spectral changes. Such significant spectral changes have been exploited in the detection of important biomolecules,[4b,c,5c,f–h] their conformational changes[5c,f] and their enzymatic activities.[5g] Of the single-stranded DNAs, the pH modulation of cytosine to i-motifs under acidic conditions has also led to changes in the self-assembly of the platinum(II) complexes.[5c] In addition, the self-assembly of platinum(II) terpyridyl-based metallosupramolecular diblock copolymers mediated by pH-responsive micellization that could induce UV-vis and NIR emission spectral changes at acidic pH has also been reported.[5e]

Intracellular pH plays a crucial role in many biological processes.[9] A small deviation of the pH values may lead to cardiopulmonary and neurological diseases such as Alzheimer's disease,[10] or may be associated with the formation of solid tumours.[11] Therefore, the development of a method for the continuous monitoring of pH with high selectivity and sensitivity is of great importance. Luminescent pH sensors are advantageous over other optical sensors due to their higher sensitivity and convenience as well as the non-invasive nature of fluorescence microscopy.[12] Probes that show NIR emission are particularly

[a]*Institute of Molecular Functional Materials (Areas of Excellence Scheme, University Grants Committee, Hong Kong) and Department of Chemistry, The University of Hong Kong, Pokfulam Road, Hong Kong, P. R. China. E-mail: wwyam@hku.hk; Fax: +852 2857 1586; Tel: +852 2859 2153*

[b]*Department of Biology and Chemistry, City University of Hong Kong, Tat Chee Avenue, Kowloon, Hong Kong, P. R. China*

† Electronic supplementary information (ESI) available: Electronic absorption spectra of aqueous solutions (50 mM NaCl) of complexes **1**, **2** and **3**. Dimerization plot for a monomer–dimer equilibrium for complex **1**. Concentration-dependent UV-vis absorption spectra of complex **1** at pH 10. Changes in absorbance of complex **1** at 650 nm with seven cycles of pH switching. Emission spectra of complex **3** at 25 °C at pH 4, 7 and 10. Relative emission intensity of complex **2** in an aqueous solution (50 mM NaCl) at 755 nm against pH. Emission spectra of complex **1** (20 μM) in aqueous solution (50 mM NaCl) at different pHs at 25 °C. See DOI: 10.1039/c3sc50196e

important as low-energy radiation can increase optical transparency and lessen tissue autofluorescence.[13] Nowadays, the working principle of the NIR luminescent pH sensors is confined to the following strategies: turning on of the luminescence by blocking photoinduced electron transfer (PET) upon protonation; reduction of the effective conjugation length of the cyanine dyes upon protonation/deprotonation; or aggregation of organic dyes/platinum(II) complexes.[5e,14] The exploration of a combination of the above strategies is anticipated to lead to the development of sensors with more significant emission spectral changes in the NIR region and thus with higher sensitivity.

In view of the fact that the aggregation of terpyridylplatinum(II) complexes would lead to significant emission spectral changes in the NIR region under different stimuli,[4b–d,5] we are interested in designing water-soluble alkynylplatinum(II) terpyridine complexes that would undergo aggregation and deaggregation as well as PET over changes in pH which are in the physiological range, resulting in drastic emission spectral changes in the NIR region. Together with the interest in the search for a new class of NIR luminescent probes with emission intensity resistant to self-quenching upon aggregation, in contrast to those commonly found in the reported pH-responsive NIR luminescent probes,[14] herein we report the synthesis and investigation of the spectral changes of the water-soluble alkynylplatinum(II) terpyridine complexes shown in Scheme 1 with pH, as well as their *in vitro* pH response and potential application in biological imaging.

Results and discussion

Synthesis, characterization, photophysical and electrochemical studies of the complexes

Water-soluble alkynylplatinum(II) terpyridine complexes **1–3** were synthesized by dehydrohalogenation reactions of $[Pt\{tpy(C_6H_4CH_2NMe_3\text{-}4)\text{-}4'\}Cl](OTf)_2$[2,4c,15] with the corresponding functionalized alkynes using modifications of a literature procedure for $[Pt(tpy)(C{\equiv}CC_6H_5)](OTf)$.[3a,16] The complexes were purified by recrystallization *via* the slow diffusion of diethyl ether vapour into methanol–acetonitrile solution mixtures of the complexes. All the complexes have been successfully characterized by ^1H and $^{13}C\{^1H\}$ NMR, IR, FAB-MS and elemental analysis. Details of the synthesis and characterization data are included in the ESI.†

The electronic absorption spectra of complexes **1–3** in dimethylformamide solution reveal intense electronic absorptions at 274–354 nm and lower-energy absorptions at *ca.* 408–496 nm (Table 1; Fig. S1 in ESI†). According to previous spectroscopic work on alkynylplatinum(II) terpyridine complexes,[4,5] the intense absorptions are ascribed to the intraligand (IL) $\pi \rightarrow \pi^*$ transitions of the alkynyl and the terpyridine ligands, whereas the lower-energy absorptions are tentatively assigned as the admixtures of $d\pi(Pt) \rightarrow \pi^*(tpy)$ metal-to-ligand charge transfer (MLCT) and alkynyl-to-terpyridine ligand-to-ligand charge transfer (LLCT) transitions. In addition, upon light excitation, complexes **1**, **2** and **3** in acetonitrile–methanol solution mixture (5 : 1, v/v) are found to emit at 582, 624 and 654 nm respectively, while in dimethylformamide solution complex **3** shows an emission centred at 634 nm (Table 1). Taken into account the microsecond lifetime and the large Stokes shift of the emission, it is likely that the emission originates from a triplet metal-to-ligand charge transfer (^{3}MLCT) ($^3[d\pi(Pt) \rightarrow \pi^*(tpy)]$) excited state with mixing of a triplet ligand-to-ligand charge transfer (^{3}LLCT) ($^3[\pi(C{\equiv}C\text{–}R) \rightarrow \pi^*(tpy)]$) character, typical of alkynylplatinum(II) terpyridine complexes.[4,5] Complexes **1–3** in the solid state show low-energy emissions ranging from 716 to 759 nm at 298 K, and the emissions are found to show significant red shifts upon cooling to 77 K (Table 1). It is likely that these low-energy solid-state emissions of the complexes are derived from triplet metal-metal-to-ligand charge transfer (^{3}MMLCT) excited states resulting from the formation of Pt···Pt and/or π–π interactions in the solid lattice.[4,6c] Lattice contraction of the complexes upon cooling to 77 K would result in stronger Pt···Pt and π–π interactions, leading to the shift of the ^{3}MMLCT emission to lower energies.[4,6c]

The electrochemical data of complexes **1–3** in dimethylformamide with 0.1 M $^nBu_4NPF_6$ as supporting electrolyte have been summarized in Table S1.† The cyclic voltammograms of complexes **1–3** display two quasi-reversible reduction couples at $E_{1/2} = -0.77$ to -0.83 V and -1.33 to -1.34 V *vs.* SCE and an irreversible oxidation wave at $E_{pa} = +0.84$ to $+1.29$ V *vs.* SCE, which are tentatively assigned as the successive one-electron reductions of the terpyridine ligands of the complexes, and the metal-centred/alkynyl ligand-centred oxidation respectively.[3a,6c,8] In addition, all the complexes show an irreversible reduction wave at $E_{pc} = -1.23$ to -1.25 V *vs.* SCE (Table S1†), which is likely attributed to the 4-{(trimethylammonium)methyl}benzene-based reduction of the substituted terpyridine ligand.[17] For complexes **1** and **2** which contain phenolic proton(s), irreversible oxidation waves at $E_{pa} = +0.97$ and $+0.73$ V *vs.* SCE, respectively, were found in their cyclic voltammograms recorded in dimethylformamide solution, while the solutions of complexes **1** and **2** in dimethylformamide in the presence of $^nBu_4NOH$ show irreversible oxidation waves at $E_{pa} = +0.61$ and $+0.55$ V *vs.* SCE respectively. It is likely that these irreversible oxidation waves are derived from the oxidations of the phenolic moieties, typical of those reported in the literature.[18] The shift of the potentials for the irreversible oxidation waves to less positive values in the presence of $^nBu_4NOH$ can be rationalized by the deprotonation of the phenolic proton(s).

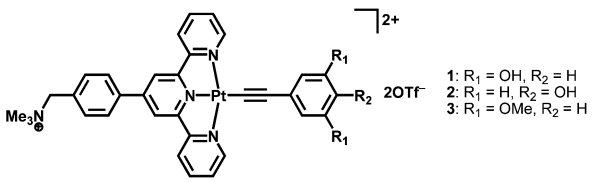

Scheme 1 Chemical structures of complexes **1–3**.

Aggregation studies of the complexes in aqueous solutions at different pHs

The ^1H NMR spectra of complex **1** in D_2O are shown in Fig. 1. At pH 4, the terpyridine proton signals are found to be poorly

Table 1 Photophysical data of complexes **1–3**

Complex	Medium (T/K)	Electronic absorption, λ/nm (ε/dm^3 mol^{-1} cm^{-1})	Emission, λ_{em}/nm (τ_0/μs)[a]
1	DMF (298)	274 (44 870), 290 (44 870), 314 (29 210), 326 (23 050), 340 (18 200), 352 (15 140), 422 (6660), 472 (5840)	—[b]
	CH_3CN–CH_3OH (5 : 1, v/v) (298)	272 (30 300), 290 (33 480), 309 (18 380), 328 (11 170), 342 (8910), 419 (3990), 465 (3670), 512 sh (1000)	582 (0.2)
	pH 7 aqueous solution[c] (298)	262 (29 490), 293 (24 720), 330 (14 810), 382 (7400), 457 (5630), 587 (2160), 663 (600)	788 (0.1)
	pH 3 aqueous solution[c] (298)	262 (28 740), 297 (23 130), 330 (14 500), 353 (10 980), 457 (5410), 587 (1970), 663 (610)	795 (0.1)
	pH 10 aqueous solution[c] (298)	230 (28 740), 276 (22 440), 323 (15 000), 351 (10 930), 471 (4990), 628 (1650)	—[b]
	Solid (298)		737 (<0.1)
	Solid (77)		758 (0.2)
2	DMF (298)	274 (66 330), 290 (60 210), 310 (36 820), 336 (21 190), 354 (14 420), 382 (6820), 408 (6750), 496 (5940)	—[b]
	CH_3CN–CH_3OH (5 : 1, v/v) (298)	274 (20 790), 310 (9790), 331 (5890), 345 (4520), 408 (1760), 480 (1620)	624 (0.2)
	pH 7 aqueous solution[c] (298)	261 (27 150), 297 (21 230), 324 (12 180), 334 (10 520), 484 (3630), 580 (1670)	750 (0.1)
	pH 3 aqueous solution[c] (298)	261 (27 620), 298 (21 100), 325 (12 370), 387 (4450), 484 (3690), 580 (1720)	755 (0.1)
	pH 10 aqueous solution[c] (298)	285 (26 240), 305 (19 360), 333 (12 450), 406 (3650), 529 (2450), 700 (910)	—[b]
	Solid (298)		716 (0.1)
	Solid (77)		755 (0.2)
3	DMF (298)	278 (56 040), 290 (53 870), 310 (31 590), 348 (14 310), 426 (6130), 464 (5720)	634 (0.1)
	CH_3CN–CH_3OH (5 : 1, v/v) (298)	264 (26 020), 270 (26 300), 290 (27 600), 309 (16 590), 330 (10 390), 344 (8520), 453 (3380), 505 sh (960)	654 (0.1)
	pH 7 aqueous solution[c] (298)	269 (23 140), 287 (19 440), 298 (16 470), 306 (14 040), 336 (8240), 347 (6910), 456 (3680), 575 (1220)	788 (<0.1)
	pH 3 aqueous solution[c] (298)	269 (23 250), 287 (19 690), 298 (16 660), 306 (14 250), 336 (8380), 347 (7050), 456 (3710), 575 (1220)	788 (<0.1)
	pH 10 aqueous solution[c] (298)	269 (23 350), 287 (19 750), 298 (16 700), 306 (14 300), 336 (8450), 347 (7050), 456 (3710), 575 (1220)	788 (<0.1)
	Solid (298)		759 (0.1)
	Solid (77)		791 (0.3)

[a] Emission lifetimes were recorded with ± 10% uncertainty. [b] Non-emissive. [c] Concentration of the complexes in aqueous solution (50 mM NaCl) was 200 μM.

resolved at 20 °C, but become much better resolved at elevated temperatures (Fig. 1a). With reference to the previous study of alkynylplatinum(II) terpyridine complexes,[5b] it is likely that in aqueous solution at pH 4 complex **1** would aggregate at 20 °C through metal–metal and/or π–π interactions and would undergo deaggregation at higher temperatures. Similarly, for the ^{1}H NMR spectra of complex **1** in D_2O at pH 10 (Fig. 1b), the terpyridine proton signals are found to be better resolved at elevated temperatures, suggesting that deaggregation has occurred. Interestingly, the terpyridine proton signals at pH 10 are found to be less broadened compared to those at pH 4 (Fig. 1b), indicating that in aqueous solution complex **1** shows a higher degree of aggregation at pH 4 than at pH 10. It is conceivable that deprotonation of the phenolic protons of

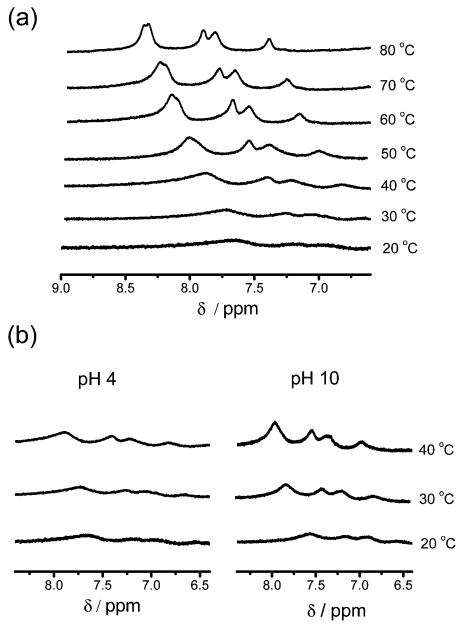

Fig. 1 (a) ^{1}H NMR spectra of complex **1** (200 μM) in D_2O with 50 mM NaCl at pH 4 at different temperatures. (b) ^{1}H NMR spectra of complex **1** (200 μM) in D_2O with 50 mM NaCl at pH 4 and pH 10 at different temperatures. The pH values are adjusted by the addition of 0.02 M HCl and 0.02 M NaOH in D_2O.

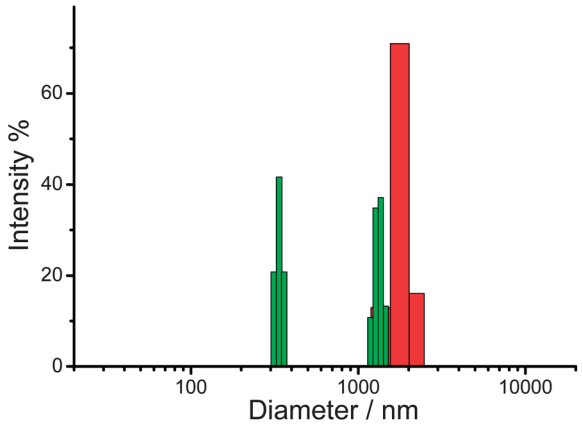

Fig. 2 Dynamic light scattering (DLS) experiments of complex **1** (200 μM) in aqueous solution (50 mM NaCl) at 25 °C at pH 4 (red) and pH 10 (green).

complex **1** at high pH leads to an increase in the hydrophilicity of the complex and hence its deaggregation in aqueous medium. This is supported by the ^{1}H NMR spectra of complex **2**, which has one less phenolic proton than complex **1**. The terpyridine proton signals of complex **2** in D_2O are also less broadened at higher temperatures and pH. This suggests that in aqueous solution complex **2** would show a lower degree of aggregation at high temperatures, typical of alkynylplatinum(II) terpyridine complexes,[5b] and that deprotonation of the phenolic proton at high pH would lead to an increase in the hydrophilicity of complex **2** and its deaggregation in aqueous medium.

The aggregation process of complex **1** in aqueous solution at different pHs has also been studied by dynamic light scattering (DLS) experiments (Fig. 2). A number-averaged hydrodynamic diameter (D_h) of *ca.* 1.8 μm was found in pH 4 aqueous solution of complex **1**, while the DLS experiment of complex **1** at pH 10 revealed a smaller value (*ca.* 1.3 μm) with lower signal intensity. Moreover, an even smaller particle size (D_h of *ca.* 0.3 μm) was observed in the pH 10 solution of complex **1** (Fig. 2). Based on the finding of large particles in μm range in both the pH 4 and 10 aqueous solutions, complex **1** would undergo aggregation with the formation of Pt···Pt and/or π–π interactions in the aqueous solutions. However, the degree of aggregation of complex **1** at pH 10 is probably lower than that at pH 4, as suggested by the smaller D_h value and the lower intensity of the light scattering signal of the large aggregates (D_h of *ca.* 1.3 μm) and the presence of smaller particles in the solution, indicating the unfavourable formation of aggregates of complex **1**.

The ground-state aggregation/deaggregation of complex **1** in aqueous solution at different pHs has been further investigated by UV-vis absorption measurements. The electronic absorption spectrum of complex **1** in aqueous solution (50 mM NaCl) at pH 4 shows an intense absorption band at 465 nm and a lower-energy absorption feature at 600 nm and is shown in Fig. S2.† According to previous spectroscopic work on alkynylplatinum(II) terpyridine complexes[4,5] and the corresponding studies in dimethylformamide solution, the absorption band at 465 nm is tentatively assigned as admixtures of dπ(Pt) → π*(tpy) MLCT and alkynyl-to-terpyridine LLCT transitions. The lower-energy absorption at 600 nm, which is absent in dimethylformamide solution, is found to show a decrease in absorbance upon an increase in temperature (Fig. S3a†). On the other hand, a decrease in temperature would lead to the growth of the absorption at 600 nm and a drop in the MLCT absorption, which is reversible for at least six repeated cycles (Fig. S3b†). As supported by ^{1}H NMR and DLS studies (*vide supra*), the absorption centred at 600 nm should originate from metal-metal-to-ligand charge transfer (MMLCT) transitions, associated with metal–metal and/or π–π interactions. The aggregation of complex **1** in aqueous solution (50 mM NaCl) at pH 4 is supported by concentration-dependent UV-vis absorption studies, where the low-energy absorption tail at 670 nm does not follow Beer's law (Fig. 3). This suggests that ground-state aggregation of the complex molecules occurred in the pH 4 solution at high concentrations of complex **1**, resulting in Pt··· Pt and/or π–π interactions and hence the MMLCT absorption. With reference to the dimerization model of platinum(II) terpyridine complexes reported in the literature,[2a] the dimerization equilibrium constants of complex **1** in pH 4 aqueous solution due to metal–metal and π–π interactions, K_{MM} and $K_{\pi\pi}$, are estimated to be 3.84×10^5 and 1.65×10^5 M respectively from the dimerization plot (Fig. S4†).

The electronic absorption spectrum of complex **1** at pH 10 (Fig. S2†) shows an absorption band at 480 nm and a broad absorption tail at 650 nm. The absorption at 480 nm is similarly assigned to MLCT transitions, while the absorption tail at 650 nm, which is more intense at temperatures lower than 20 °C but weaker at higher temperatures (Fig. S5†), should originate from MMLCT transitions through metal–metal and/or π–π interactions. Interestingly, the MMLCT absorption at pH 10 is

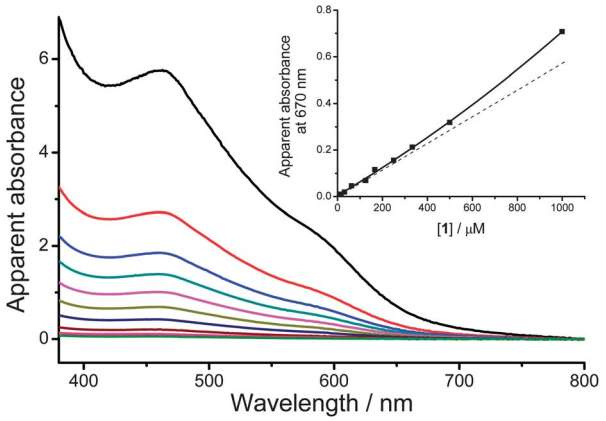

Fig. 3 Concentration-dependent UV-vis absorption spectra of complex **1** in aqueous solution (50 mM NaCl) at pH 4. Apparent absorbance refers to the absorbance value corrected to 1 cm path length equivalence. Inset shows the plot of apparent absorbance at 670 nm against concentration of complex **1**.

red-shifted compared to that at pH 4, which should not be due to stronger aggregation at pH 10 as suggested from the ^{1}H NMR spectra of complex **1** in D_2O at pH 4 and 10 (Fig. 1b), the DLS experiments of complex **1** in pH 10 aqueous solution (Fig. 2) and the smaller changes in the MMLCT absorption with temperature at pH 10 (Fig. S3a and S5†). Instead, it is likely that the red shift is due to deprotonation of the phenolic protons of complex **1** at pH 10, that will lead to a stronger electron-donating effect of the alkynyl ligand, and hence a rise of the energy of the dπ(Pt) orbital. Similar shifts of the absorption band to the red with an increase in pH have been reported previously.[4a] The smaller extent of aggregation of complex **1** in pH 10 aqueous solution is further supported by the results from concentration-dependent electronic absorption study of the complex in pH 10 aqueous solution, which shows a low-energy absorption tail at 750 nm that follows Beer's law (Fig. S6†). This may probably be due to the small association constant of the complex molecules in aqueous solution at pH 10. It is worth noting that the aggregation and deaggregation of complex **1** in aqueous solution have been found to be reversible over at least seven cycles of pH switching between 4 and 10, as monitored by the changes in MMLCT absorption of complex **1** at 650 nm (Fig. S7†). For the UV-vis absorption spectrum of complex **1** at pH 7 (Fig. S2†), the absorption bands at 465 and 600 nm are assigned as MLCT/LLCT and MMLCT transitions, respectively, similar to that at pH 4. The weaker MMLCT absorption also indicates that complex **1** is less aggregated at pH 7 than at pH 4.

With reference to the UV-vis absorption spectra of complex **1** at different pHs and at different temperatures (Fig. S2–S5†) and the ^{1}H NMR spectra of the terpyridine protons of complex **2** in D_2O, the electronic absorption features of complex **2** in aqueous solution (50 mM NaCl) at both pH 4 and 7 centred at 488 and 585 nm as well as those at pH 10 centred at 498 and 600 nm are similarly assigned as the respective MLCT/LLCT and MMLCT transitions (Fig. S8–S10†). The red shift of the MLCT/LLCT and MMLCT absorptions at pH 10 is also ascribed to the deprotonation of the phenolic proton in complex **2**. On the other hand, the MLCT/LLCT and MMLCT absorption characteristics of an aqueous solution (50 mM NaCl) of complex **3**, with methoxy substituent on the alkynyl ligand instead of phenolic protons in complexes **1** and **2**, at 457 and 580 nm (Fig. S11 and S12†) are both found to be unchanged at different pHs (Fig. S11†). This suggests that the aggregation and deaggregation processes of complexes **1** and **2** are modulated by the acid-base behaviour of their phenolic protons. Deprotonation of the phenolic protons in complexes **1** and **2** would occur at higher pH, which would make the complexes more hydrophilic in nature, leading to the deaggregation of the complexes in aqueous medium.

NIR emission spectral changes of the complexes in aqueous solutions over physiological pH

The emission spectra of complex **1** in aqueous solution (50 mM NaCl) at various pH values have been recorded by excitation at 480 nm (Fig. 4). At pH 4, an NIR emission band centred at 795 nm is observed, which is found to diminish at higher temperature (Fig. 5). Although non-radiative decay would be more efficient at higher temperature, such a drastic decrease in the emission at 795 nm (the emission at 80 °C was *ca.* 18% of that at 15 °C) cannot simply be accounted for by enhanced non-radiative decay alone. Together with the observation of the emission in the NIR region, the emission is most likely attributed to the aggregation of the complex **1** molecules through

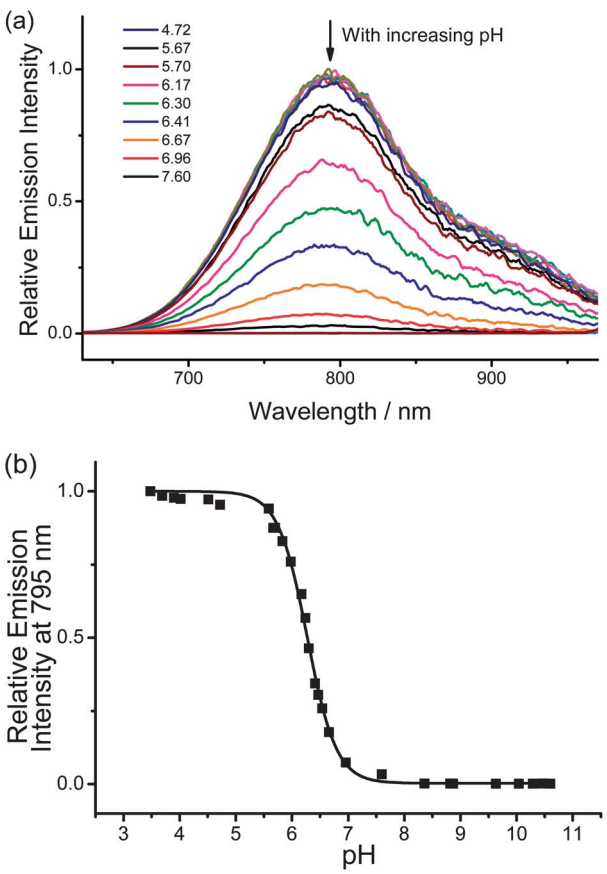

Fig. 4 (a) Emission spectra of complex **1** (200 μM) in aqueous solution (50 mM NaCl) at various pH values at 25 °C. λ_{ex} = 480 nm. (b) A plot of relative emission intensity of complex **1** at 795 nm *versus* pH.

metal–metal and/or π–π interactions, where the d_{z^2} orbitals on the platinum atoms of the complex molecules would overlap with each other. This results in the formation of dσ and dσ* orbitals, leading to the ^{3}MMLCT emission. At higher temperature, deaggregation probably occurs, and hence a significant decrease in the low-energy emission is found.

The emission intensity is relatively unchanged from pH 3.5 to 5.6. However, upon an increase in pH above 5.6, the NIR emission shows a significant drop in intensity and becomes completely "turned-off" at or above pH 7.6. In view of the aggregation/deaggregation of complex **1** at different pHs as suggested from the ^{1}H NMR, DLS and UV-vis absorption studies (Fig. 1–3 and S1–S6†), the decrease in the NIR emission intensity has been ascribed to the deprotonation of the phenolic protons of complex **1**, whose pK_a* is determined to be 6.27 from the emission spectral changes with pH (Fig. 4b).[19] It is likely that the deprotonation leads to an increase in the hydrophilicity of complex **1**, causing deaggregation of the complex, and hence a drop in its ^{3}MMLCT emission intensity. This has further been supported by a lack of pH-dependence of the NIR emission of an aqueous solution of the control complex, **3**, at 788 nm (Fig. S13†). On the other hand, the NIR emission of an aqueous solution of complex **2** centred at 755 nm is found to diminish at higher pH (Fig. S14†), similar to the spectral changes of complex **1**. However, the spectral changes of complex **2** are much smaller than those of complex **1**, possibly due to the presence of only one phenolic proton in complex **2**. Therefore, the change in hydrophilicity of complex **2** after deprotonation (pK_a* determined to be 7.71 from the emission spectral changes with pH, Fig. S14†) is not as significant as that in complex **1**, leading to a smaller decrease in the ^{3}MMLCT emission intensity at higher pH.

In addition, the complete "turning-off" of the NIR emission of complex **1** at high pH, which is not commonly observed in the reported deaggregation of platinum(II) terpyridine complexes,[5b,d,e] may suggest the presence of an additional quenching pathway. Based on the electrochemical data of complex **1** (Table S1†) and the zero–zero transition energy, E_{0-0}, determined to be 1.84 eV from the intersection of the electronic absorption and emission spectra of complex **1** in aqueous solution (50 mM NaCl), the Gibbs free energy change of the PET from the phenolic moiety of the alkynyl ligand, ΔG, is estimated to be −0.06 and −0.42 eV in neutral and basic solution respectively. This indicates that PET would be energetically more favourable to occur in basic solution, probably due to the deprotonation of the phenolic groups on the alkynyl ligand of complex **1** which becomes more electron-rich. With a combination of aggregation/deaggregation of platinum(II) complex moieties and PET, the changes in the NIR emission intensity of complex **1** with pH is found to be *ca.* 1350-fold, which is the highest ever reported value to the best of our knowledge. Such drastic changes would allow the NIR emission of complex **1** to be "off" at physiological pH (7.0–7.4) but to be "on" upon small changes of pH below 7.0, for example, in tumour cells.[11] Furthermore, although the NIR emission of complex **1** originates from aggregation of the complex moieties, the emission is relatively insensitive to the temperature below 50 °C (Fig. 5). This is probably due to the formation of strong aggregates of complex **1** in aqueous solution, requiring higher temperature to provide sufficient energy for the deaggregation. As a result, a small change in physiological temperature would not have significant interference on the detection of pH by the NIR emission spectral responses of complex **1**.

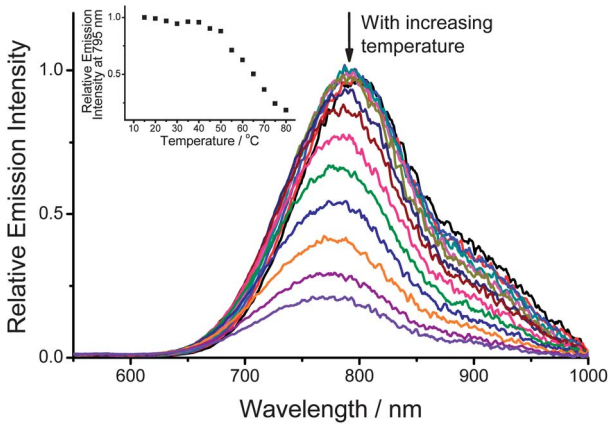

Fig. 5 Emission spectral changes of complex **1** (200 μM) in aqueous solution (50 mM NaCl) at pH 4 with temperature. λ_{ex} = 452 nm. Inset: a plot of relative emission intensity at 795 nm *versus* temperature.

Cell-imaging experiments using complex 1 as a pH-responsive NIR luminescent probe

With the promising pH response and the attractive NIR emitting feature in solution, we were prompted to investigate the potential application of complex **1** as a pH-responsive NIR luminescent probe in cell-imaging experiments. Since the ^{3}MMLCT emission of complex **1** arising from the aggregation of complex moieties could be altered by the presence of proteins and biomolecules as shown by previous studies of alkynylplatinum(II) terpyridine complexes with biomolecules in solution,[4b,c,5c,f,g,h] the effect of pH on the ^{3}MMLCT emission in cells was first studied by using Madin–Darby canine kidney (MDCK) cells fixed with methanol. Methanol fixation can result in precipitation of proteins and removal of lipids from cells,[20] and thus any observable change in ^{3}MMLCT emission intensity would not be due to the binding of complex **1** to proteins or other biomolecules. Moreover, as fixed cells have permeable membranes,[20] any difference in the emission intensity should not be ascribed to different concentrations of complex **1** in cellular compartments. Therefore, fixed-cell experiments with incubation of buffer solutions at different pHs can reveal the pH response of ^{3}MMLCT emission of complex **1** in cells. Confocal microscopy images of fixed MDCK cells incubated with 20 μM of complex **1**[21] in serum- and phenol red-free Dulbecco's modified Eagle's medium (DMEM) at 37 °C for 1 h,[22] followed by further incubation in pH 5.72 MES buffer solutions at room temperature for 10 min, revealed a strong NIR emission band at λ_{em} = 750 ± 50 nm (Fig. 6a). As fixed cells have permeable membranes,[20] the intracellular pH should be equal to the pH value of the buffer solution, suggesting that the fixed cells

incubated with complex **1** at an intracellular pH of 5.72 would show strong NIR emission. On the other hand, incubation of the fixed MDCK cells with 20 μM of complex **1** in serum- and phenol red-free DMEM at 37 °C for 1 h, followed by further incubation in pH 6.75 and 7.80 MES buffer solutions, respectively, at room temperature for 10 min, resulted in weak NIR emission (Fig. 6d and g), indicating that the observation of NIR emission is closely associated with the intracellular pH environment. A more detailed study on the NIR emission of the fixed MDCK cells incubated with 20 μM of complex **1** followed by the incubation with buffer solutions at different pH values has been performed (Fig. 7). It has been found that the NIR emission intensity of the fixed MDCK cells starts to decrease when the intracellular pH increases above 5.5, with the most significant diminution from pH 6 to 7, which is similar to the pH response of the NIR emission of complex **1** in solution described above. In addition, the NIR emission intensity of the fixed MDCK cells showed a sigmoidal relationship with the intracellular pH, with a pK_a* value determined to be 6.30, which is in good agreement with the pK_a* value of complex **1** (6.27) deduced from the emission spectral changes in solution at different pHs. As a result, the NIR emission should be ascribed to the ^{3}MMLCT emission of complex **1** inside the fixed MDCK cells. Upon an increase in intracellular pH, deprotonation of the phenolic protons in the alkynyl ligands of complex **1** would lead to an increase in the hydrophilicity of the complex, resulting in both deaggregation and PET quenching to "turn off" the ^{3}MMLCT emission, which is similar to that observed in solution

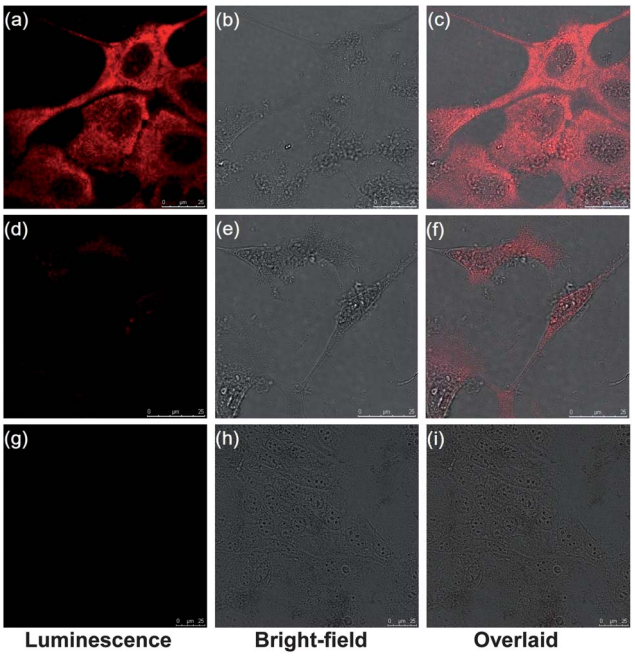

Fig. 6 Confocal microscopy images of fixed MDCK cells incubated with 20 μM of complex **1** for 1 h followed by incubation with buffer solutions of pH 5.72 (a–c), 6.75 (d–f) and 7.80 (g–i) respectively at room temperature for 10 min. λ_{ex} = 488 nm and λ_{em} = 750 ± 50 nm. Luminescence (a, d and g), bright-field (b, e and h) and overlaid (c, f and i) microscopy images are shown in the corresponding figures.

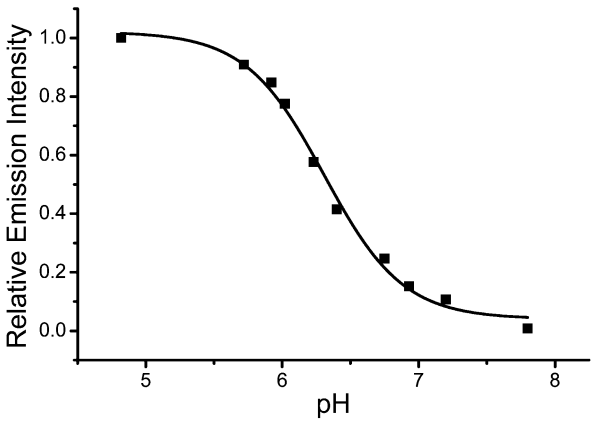

Fig. 7 Emission intensity changes of fixed MDCK cells incubated with 20 μM of complex **1** at 37 °C for 1 h followed by incubation with buffer solutions of known pH at room temperature for 10 min. The emission of fixed MDCK cells was measured by confocal microscopy with λ_{ex} = 488 nm and λ_{em} = 750 ± 50 nm.

(*vide supra*). Although the changes in the NIR emission intensity of complex **1** in the fixed cells (*ca.* 118-fold) are smaller than those in solution (*ca.* 1350-fold), probably due to the lower concentration of complex **1** in the cell-imaging experiments, the NIR emission of complex **1** in the cellular compartments still have significant changes in confocal microscopy (Fig. 6a, d and g) over pH 6 to 7, which lies in the pH range that is highly relevant to many cellular events and diseases such as tumour formation.[9–11]

The observation of pH-responsive ^{3}MMLCT emission of complex **1** in fixed MDCK cells prompted us to further study the potential application of complex **1** as a pH-responsive NIR luminescent probe for imaging acidic cellular compartments, such as lysosomes, in living cells. Confocal microscopy images of live MDCK cells incubated with 20 μM of complex **1** in serum- and phenol red-free DMEM at 37 °C for 1 h revealed a strong NIR emission at λ_{em} = 750 ± 50 nm in vesicular distribution (Fig. 8a–d). The MDCK cells remained viable after the incubation as revealed by (1) their morphology in the differential interference contrast (DIC) images and (2) the 3-(4,5-dimethyl-2-thiazolyl)-2,5-diphenyltetrazolium bromide (MTT) assay result (*ca.* 97% viability as compared to untreated MDCK cells). The NIR emission showed good co-localization with the green emission of LysoSensor Green DND-189 (as indicated by the yellow spots in the merged image), with a Mander's co-localization coefficient of 95%, where the Mander's co-localization coefficient is a measure of the fraction of NIR emission of complex **1** co-localizing with the green emission of DND-189.[23] On the other hand, MDCK cells incubated with the control complex **3**, which exhibits pH-insensitive NIR emission upon aggregation (Fig. S14†), in serum- and phenol red-free DMEM for 1 h showed NIR emission, but in a rather diffused manner with a lower degree of co-localization with DND-189 (Fig. 8e–h; Mander's co-localization coefficient = 57%). As DND-189 is known to accumulate and show stronger green emission in acidic organelles such as lysosomes, a high degree of co-localization with the strong NIR emission of complex **1** suggests that

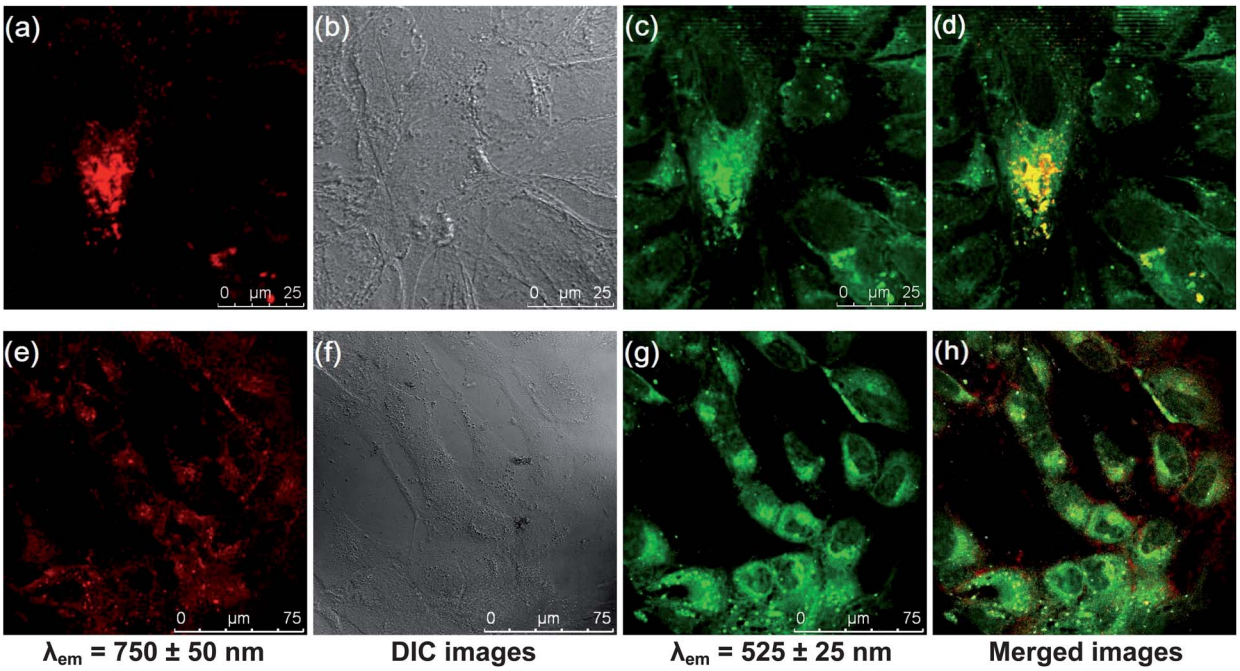

Fig. 8 Confocal microscopy images of live MDCK cells incubated with 20 μM of complex **1** for 1 h (a–d), and the microscopy images of live MDCK cells incubated with 20 μM of complex **3** for 1 h (e–h). $\lambda_{ex} = 488$ nm. Co-staining with 1 μM of DND-189 in serum- and phenol red-free DMEM was carried out 15 min prior to the imaging experiments. Luminescence images at $\lambda_{em} = 750 \pm 50$ nm (a and e), differential interference contrast (DIC) images (b and f), luminescence images at $\lambda_{em} = 525 \pm 25$ nm from the co-stained DND-189 (c and g) and the merged images of the emission at $\lambda_{em} = 750 \pm 50$ nm and 525 ± 25 nm (d and h) are shown in the corresponding figures.

the complex emission is enhanced by the low pH in the environment in a way that is similar to the observed pH-dependent emission in solution and in fixed cells. Therefore, our results showed that the emission intensity of complex **1** can be utilized to distinguish acidic lysosomes from cytoplasm and other cellular organelles, where only weak NIR emission was observed, probably due to the deaggregation of the complex moieties as well as PET quenching of the ^{3}MMLCT emission at higher pH. On the other hand, it is possible that complex **3** can label cellular organelles other than acidic lysosomes as its NIR emission is not sensitive to changes in pH, and hence a more diffused NIR emission that shows a lower degree of co-localization with DND-189 is found in the confocal microscopy images (Fig. 8e and h). This further supports that the different NIR emission intensity of complex **1** in MDCK cells is mainly due to the different pH values of the cellular compartments. With the observable changes in the NIR emission intensity in the cells, complex **1** is a promising candidate for the tracking of acidic organelles, such as lysosomes, or cellular events that involve changes over pH in the physiological range.

Conclusions

In conclusion, water-soluble alkynylplatinum(II) terpyridine complexes have been synthesized. Complexes **1** and **2** have been shown to aggregate at low pH and, upon excitation, display ^{3}MMLCT NIR emission through metal–metal and/or π–π interactions. An increase in pH above their pK_a* values would result in deprotonation of the phenolic protons of the alkynyl ligands, leading to an increase in the hydrophilicity of the complexes and hence deaggregation of the complex moieties. Due to this deaggregation, together with the occurrence of PET, the NIR emission of complex **1** is completely "turned-off" at pH above 7.6. Cell-imaging experiments with complex **1** have demonstrated its potential as an NIR luminescent probe for the tracking of cellular compartments with deviations from physiological pH, such as lysosomes. Also, the complex may be further exploited for probing intracellular events that involve pH changes.

Acknowledgements

V.W.-W.Y. acknowledges support from the University Grants Committee Areas of Excellence Scheme (AoE/P-03/08), the General Research Fund (GRF) (HKU 7064/11P) and Collaborative Research Fund (CRF) (HKUST2/CRF/10) from the Research Grants Council of Hong Kong Special Administrative Region, China. C.Y.-S.C acknowledges the receipt of a Postgraduate Studentship administered by The University of Hong Kong. Dr A. Y.-Y. Tam is acknowledged for his helpful discussions.

Notes and references

1 (*a*) R. S. Osborn and D. Rogers, *J. Chem. Soc., Dalton Trans.*, 1974, 1002; (*b*) K. W. Jennette, J. T. Gill, J. A. Sadownick and S. J. Lippard, *J. Am. Chem. Soc.*, 1976, **98**, 6159; (*c*) V. M. Miskowski and V. H. Houlding, *Inorg. Chem.*, 1991, **30**, 4446; (*d*) V. H. Houlding and V. M. Miskowski, *Coord.*

Chem. Rev., 1991, **111**, 145; (*e*) R. Büchner, C. T. Cunningham, J. S. Field, R. J. Haines, D. R. McMillin and G. C. Summerton, *J. Chem. Soc., Dalton Trans.*, 1999, 711; (*f*) V. W. W. Yam, K. M. C. Wong and N. Zhu, *J. Am. Chem. Soc.*, 2002, **124**, 6506.

2 (*a*) J. A. Bailey, M. G. Hill, R. E. Marsh, V. M. Miskowski, W. P. Schaefer and H. B. Gray, *Inorg. Chem.*, 1995, **34**, 4591; (*b*) G. T. Morgan and F. H. Burstall, *J. Chem. Soc.*, 1934, 1498; (*c*) M. Howe-Grant and S. J. Lippard, *Inorg. Synth.*, 1980, **20**, 101.

3 (*a*) V. W. W. Yam, R. P. L. Tang, K. M. C. Wong and K. K. Cheung, *Organometallics*, 2001, **20**, 4476; (*b*) W. B. Connick, L. M. Henling, R. E. Marsh and H. B. Gray, *Inorg. Chem.*, 1996, **35**, 6261; (*c*) W. B. Connick, R. E. Marsh, W. P. Schaefer and H. B. Gray, *Inorg. Chem.*, 1997, **36**, 913; (*d*) A. J. Goshe, I. M. Steele and B. Bosnich, *J. Am. Chem. Soc.*, 2003, **125**, 444; (*e*) R. Büchner, J. S. Field, R. J. Haines, C. T. Cunningham and D. R. McMillin, *Inorg. Chem.*, 1997, **36**, 3952; (*f*) R. H. Herber, M. Croft, M. J. Coyer, B. Bilash and A. Sahiner, *Inorg. Chem.*, 1994, **33**, 2422.

4 (*a*) K. M. C. Wong, W. S. Tang, X. X. Lu, N. Zhu and V. W. W. Yam, *Inorg. Chem.*, 2005, **44**, 1492; (*b*) C. Y. S. Chung and V. W. W. Yam, *J. Am. Chem. Soc.*, 2011, **133**, 18775; (*c*) C. Y. S. Chung and V. W. W. Yam, *Chem. Sci.*, 2013, **4**, 377; (*d*) S. Y. L. Leung, A. Y. Y. Tam, C. H. Tao, H. S. Chow and V. W. W. Yam, *J. Am. Chem. Soc.*, 2012, **134**, 1047.

5 (*a*) C. Yu, K. M. C. Wong, K. H. Y. Chan and V. W. W. Yam, *Angew. Chem., Int. Ed.*, 2005, **44**, 791; (*b*) V. W. W. Yam, K. H. Y. Chan, K. M. C. Wong and B. W. K. Chu, *Angew. Chem., Int. Ed.*, 2006, **45**, 6169; (*c*) C. Yu, K. H. Y. Chan, K. M. C. Wong and V. W. W. Yam, *Proc. Natl. Acad. Sci. U. S. A.*, 2006, **103**, 19652; (*d*) C. Yu, K. H. Y. Chan, K. M. C. Wong and V. W. W. Yam, *Chem.–Eur. J.*, 2008, **14**, 4577; (*e*) V. W. W. Yam, Y. C. Hu, K. H. Y. Chan and C. Y. S. Chung, *Chem. Commun.*, 2009, 6216; (*f*) M. C. L. Yeung, K. M. C. Wong, Y. K. T. Tsang and V. W. W. Yam, *Chem. Commun.*, 2010, **46**, 7709; (*g*) C. Y. S. Chung, K. H. Y. Chan and V. W. W. Yam, *Chem. Commun.*, 2011, **47**, 2000; (*h*) M. C. L. Yeung and V. W. W. Yam, *Chem.–Eur. J.*, 2011, **17**, 11987.

6 (*a*) H. K. Yip, C. M. Che and T. C. W. Mak, *J. Chem. Soc., Chem. Commun.*, 1992, 1369; (*b*) J. A. Bailey, V. M. Miskowski and H. B. Gray, *Inorg. Chem.*, 1993, **32**, 369; (*c*) H. K. Yip, L. K. Cheng, K. K. Cheung and C. M. Che, *J. Chem. Soc., Dalton Trans.*, 1993, 2933; (*d*) M. G. Hill, J. A. Bailey, V. M. Miskowski and H. B. Gray, *Inorg. Chem.*, 1996, **35**, 4585.

7 (*a*) F. Camerel, R. Ziessel, B. Donnio, C. Bourgogne, D. Guillon, M. Schmutz, C. Iacovita and J. P. Bucher, *Angew. Chem., Int. Ed.*, 2007, **46**, 2659; (*b*) M. Y. Yuen, V. A. L. Roy, W. Lu, S. C. F. Kui, G. S. M. Tong, M. H. So, S. S. Y. Chui, M. Muccini, J. Q. Ning, S. J. Xu and C. M. Che, *Angew. Chem., Int. Ed.*, 2008, **47**, 9895; (*c*) C. Po, A. Y. Y. Tam, K. M. C. Wong and V. W. W. Yam, *J. Am. Chem. Soc.*, 2011, **133**, 12136.

8 (*a*) T. J. Wadas, Q. M. Wang, Y. J. Kim, C. Flaschenreim, T. N. Blanton and R. Eisenberg, *J. Am. Chem. Soc.*, 2004, **126**, 16841; (*b*) S. Chakraborty, T. J. Wadas, H. Hester, C. Fiaschenreim, R. Schmehl and R. Eisenberg, *Inorg. Chem.*, 2005, **44**, 6284; (*c*) S. Chakraborty, T. J. Wadas, H. Hester, R. Schmehl and R. Eisenberg, *Inorg. Chem.*, 2005, **44**, 6865.

9 (*a*) I. Yuli and A. Oplatka, *Science*, 1987, **235**, 340; (*b*) P. Donoso, M. Beltrán and C. Hidalgo, *Biochemistry*, 1996, **35**, 13419; (*c*) R. A. Gottlieb and A. Dosanjh, *Proc. Natl. Acad. Sci. U. S. A.*, 1996, **93**, 3587; (*d*) V. A. Golovina and M. P. Blaustein, *Science*, 1997, **275**, 1643; (*e*) H. A. Clark, R. Kopelman, R. Tjalkens and M. A. Philbert, *Anal. Chem.*, 1999, **71**, 4837.

10 (*a*) D. A. Russell, R. H. Pottier and D. P. Valenzeno, *Photochem. Photobiol.*, 1994, **59**, 309; (*b*) D. Lagadic-Gossmann, M. Rissel, M. Galisteo and A. Guillouzo, *Br. J. Pharmacol.*, 1999, **128**, 1673; (*c*) M. G. Cogan, *Fluid and Electrolytes*, Appleton and Lange-Prentice Hall Publishers, Norwalk, CT, 1991.

11 (*a*) R. J. Gillies, N. Raghunand, M. L. Garcia-Martin and R. A. Gatenby, *IEEE Eng. Med. Biol. Mag.*, 2004, **23**, 57; (*b*) G. Helmlinger, F. Yuan, M. Dellian and R. K. Jain, *Nat. Med.*, 1997, **3**, 177.

12 H. R. Kermis, Y. Kostov, P. Harms and G. Rao, *Biotechnol. Prog.*, 2002, **18**, 1047.

13 (*a*) E. Soini and I. Hemmila, *Clin. Chem.*, 1979, **25**, 353; (*b*) K. Licha, *Top. Curr. Chem.*, 2002, **222**, 1; (*c*) P. W. Barone, S. Baik, D. A. Heller and M. S. Strano, *Nat. Mater.*, 2005, **4**, 86; (*d*) A. N. Bashkatov, E. A. Genina, V. I. Kochubey and V. V. Tuchin, *J. Phys. D: Appl. Phys.*, 2005, **38**, 2543.

14 (*a*) Z. J. Myng and P. Gabor, *Anal. Chem.*, 1991, **63**, 2934; (*b*) M. S. Briggs, D. D. Burns, M. E. Cooper and S. J. Gregory, *Chem. Commun.*, 2000, 2323; (*c*) O. Finikova, A. Galkin, V. Rozhkov, M. Cordero, C. Hägerhäll and S. Vinogradov, *J. Am. Chem. Soc.*, 2003, **125**, 4882; (*d*) Z. Zhang and S. Achilefu, *Chem. Commun.*, 2005, 5887; (*e*) S. A. Hilderbrand and R. Weissleder, *Chem. Commun.*, 2007, 2747; (*f*) B. Tang, X. Liu, K. H. Xu, H. Huang, G. W. Yang and L. G. An, *Chem. Commun.*, 2007, 3726; (*g*) A. Almutairi, S. J. Guillaudeu, M. Y. Berezin, S. Achilefu and J. M. J. Fréchet, *J. Am. Chem. Soc.*, 2008, **130**, 444; (*h*) B. Tang, F. Yu, P. Li, L. Tong, X. Duan, T. Xie and X. Wang, *J. Am. Chem. Soc.*, 2009, **131**, 3016; (*i*) S. Thyagarajan, T. Leiding, S. P. Årsköld, A. V. Cheprakov and S. A. Vinogradov, *Inorg. Chem.*, 2010, **49**, 9909; (*j*) H. Lu, B. Xu, Y. Dong, F. Chen, Y. Li, Z. Li, J. He, H. Li and W. Tian, *Langmuir*, 2010, **26**, 6838; (*k*) P. Song, X. Chen, Y. Xiang, L. Huang, Z. Zhou, R. Wei and A. Tong, *J. Mater. Chem.*, 2011, **21**, 13470; (*l*) S. Chen, J. Liu, Y. Liu, H. Su, Y. Hong, C. K. W. Jim, R. T. K. Kwok, N. Zhao, W. Qin, J. W. Y. Lam, K. S. Wong and B. Z. Tang, *Chem. Sci.*, 2012, **3**, 1804.

15 J. T. Wang, Y. Li, J. H. Tan, L. N. Jia and Z. W. Mao, *Dalton Trans.*, 2011, **40**, 564.

16 (*a*) K. Sonogashira, S. Takahashi and N. Hagihara, *Macromolecules*, 1977, **10**, 879; (*b*) S. Takahashi, M. Kariya, T. Yakate, K. Sonogashira and N. Hagihara, *Macromolecules*, 1978, **11**, 1063; (*c*) V. W. W. Yam,

C. H. Tao, L. Zhang, K. M. C. Wong and K. K. Cheung, *Organometallics*, 2001, **20**, 453.

17 (*a*) S. F. Nelsen and P. J. Hintz, *J. Am. Chem. Soc.*, 1972, **94**, 7114; (*b*) A. K. Kontturi, K. Kontturi, L. Murtomaki and D. J. Schiffrin, *Acta Chem. Scand.*, 1992, **46**, 47; (*c*) J. F. Michalec, S. A. Bejune, D. G. Cuttel, G. C. Summerton, J. A. Gertenbach, J. S. Field, R. J. Haines and D. R. McMillin, *Inorg. Chem.*, 2001, **40**, 2193.

18 (*a*) S. V. Jovanovic, M. Tosic and M. G. Simic, *J. Phys. Chem.*, 1991, **95**, 10824; (*b*) J. D. Roger, W. Jedral and N. J. Bunce, *Environ. Sci. Technol.*, 1999, **33**, 1453.

19 Although a number of reported studies defined the acid dissociation constant obtained from the emission measurement as pK_a (ref. 14*b*, *d*–*h*), we prefer to report this value as pK_a* due to the fact that the emission spectral changes with pH are related to the excited state of the complex molecules.

20 (*a*) J. Epstein, H. Xiao and B. K. Oba, *Blood*, 1989, **74**, 913; (*b*) A. A. Pollice, J. P. McCoy, Jr, S. E. Shackney, C. A. Smith, J. Agarwal, D. R. Burholt, L. E. Janocko, F. J. Hornicek, S. G. Singh and R. J. Hartsock, *Cytometry*, 1992, **13**, 432; (*c*) M. Dasari, S. Lee, J. Sy, D. Kim, S. Lee, M. Brown, M. Davis and N. Murthy, *Org. Lett.*, 2010, **12**, 3300; (*d*) U. Schnell, F. Dijk, K. A. Sjollema and B. N. G. Giepmans, *Nat. Methods*, 2012, **9**, 152.

21 Lower dosage of complex **1** (20 μM) was employed in the cell-imaging experiments, as it is generally more favourable. Emission spectrum of complex **1** (20 μM) in aqueous solution (50 mM NaCl) revealed a NIR emission band centred at 780 nm (Fig. S15†), which is tentatively assigned as ^{3}MMLCT emission. This suggests that complex **1** can still undergo aggregation with Pt···Pt and π–π interactions at such a low concentration. Moreover, the ^{3}MMLCT emission intensity was found to be sensitive to pH changes (Fig. S15b†), similar to the study of complex **1** in aqueous solution at 200 μM with pH. Also, from the DLS experiments, complex **1** (20 μM) was found to form aggregates with D_h of 210 and 160 nm in 50 mM aqueous NaCl solution at pH 4 and 10, respectively (Fig. S16†). We believe that these smaller aggregates would favour uptake by live cells.

22 Serum- and phenol red-free DMEM was used during the incubation of MDCK cells with complexes **1** and **3** and LysoSensor DND-189, as well as further incubation, if needed, after the loading of MDCK cells with complexes **1** and **3** in order to prevent any interference on the emission of the complexes and DND-189 by the serum proteins and phenol red dye.

23 K. W. Dunn, M. M. Kamocka and J. H. McDonald, *Am. J. Physiol.: Cell Physiol.*, 2011, **300**, C723–C742.

